JOURNAL OF APPLIED ELECTROCHEMISTRY 21 (1991) 716–720

Effect of anode material and bath composition on bubble layer resistivity and gaseous volume fraction in an aluminium electrolysis cell with sloping anode and cathode

D. KASHERMAN*, M. SKYLLAS-KAZACOS

School of Chemical Engineering and Industrial Chemistry, University of New South Wales, Kensington, N.S.W. 2033, Australia

Received 8 November 1990; revised 11 February 1991

Two carbon anodes of different formulation were employed to study the effect of varying anode–cathode distance (*ACD*) on the effective bath resistivity in a laboratory cell that utilized a sloping inert-wettable TiB_2-carbon composite cathode and sloping anode. The bubble layer resistivity and gaseous volume fraction values were also determined and were employed to verify the observed changes in the bubble contribution to the effective bath resistivity. Results associated with the addition of excess AlF_3 and NaCl to the bath are also included and discussed.

1. Introduction

In previous papers [1, 2], we have shown how a reduction in ACD (anode–cathode distance) can influence the effective bath resistivity and thus the energy efficiency of an aluminium electrolysis cell. This effect is very important in determining the viable operating *ACD* giving the optimum energy saving as offered by a new aluminium electrolysis cell with a wettable inert cathode [3–5]. In a separate paper [6], it was shown that bubble layer resistivity and gaseous volume fraction can be estimated from the effective bath resistance data obtained in a laboratory cell with a sloping inert cathode and sloping ATJ graphite anode. It is well known that different anode carbon materials can have different interfacial properties [5, 7], which can have a dramatic influence on bubble size. Bubble size in turn affects the effective bath resistivity in the electrolysis cell [8]. In the present paper, effective bath resistance values were determined for baked carbon anodes under similar operating conditions as employed in the previous study of graphite [1, 2, 6].

2. Experimental details

The experimental set-up and electrode design used in this study was described in detail earlier [1, 2, 6]. The electrodes employed had a 12° angle of inclination, the cathode being fabricated from a TiB_2-carbon composite disc. Two carbon anodes of different formulation with the same coke and pitch raw materials were employed in this study (supplied by Comalco Research Centre, Australia).

The first anode, referred to as Type I had the optimum granulometry (optimized from the vibration bulk density data) and the optimum pitch content (optimized from the apparent density of filler data). The second anode, Type II, had 50% fines fraction, also with its optimum pitch level. This anode appeared to be more porous than the Type I material, and the carbon particles on the surface could easily be rubbed-off. The BET surface areas were $0.40\,m^2\,g^{-1}$ and $0.65\,m^2\,g^{-1}$ for Type I and Type II, respectively.

A HP 6261B power supply was employed to deliver the constant current during the measurements, while the steady state potential was recorded on a Riken Denshi D8DG XY recorder as well as measured by a HP 3465B digital voltmeter. Anodic reaction overvoltage values were obtained from previously measured data at the corresponding current density [9]. These overvoltage data showed that anode Type II gives a lower overvoltage than that of anode Type I at a given current density.

3. Results and discussion

3.1. *Effect of anode materials*

The bath resistivity at each *ACD* was calculated from the cell potential data and by following the equations outlined previously [6]. The values of bath resistivity (assuming the geometric surface area is the effective surface area and is constant with respect to *ACD*) are summarized in Tables 1 and 2 at various bath compositions. These results indicate that the effective bath resistivity increases as ACD is reduced. There is a big

* Now at Century-Yuasa Batteries Pty, Ltd., P.O. Box 427, Goodna, Queensland 4300, Australia.

0021-891X/91 $03.00 + .12

Table 1. Bath resistivity (Ω cm) at $[Al_2O_3]$ = 7.5 wt %, CR = 3.0, and T = 985° C.

Electrode ACD (cm)	Type I		Type II	
	Plain*	NaCl†	Plain*	NaCl†
0.2	3.20	2.93	2.71	2.36
0.5	1.37	1.27	1.14	1.09
0.8	0.96	0.86	0.82	0.79
1.0	0.79	0.79	0.70	0.66
1.2	0.74	0.70	0.63	0.59
1.5	0.63	0.57	0.54	0.50
2.0	0.53	0.48	0.45	0.42
2.5	0.45	0.41	0.42	0.39
3.0	0.42	0.40	0.42	0.38

* Plain = No additive.
† NaCl = 5.5 wt % NaCl.

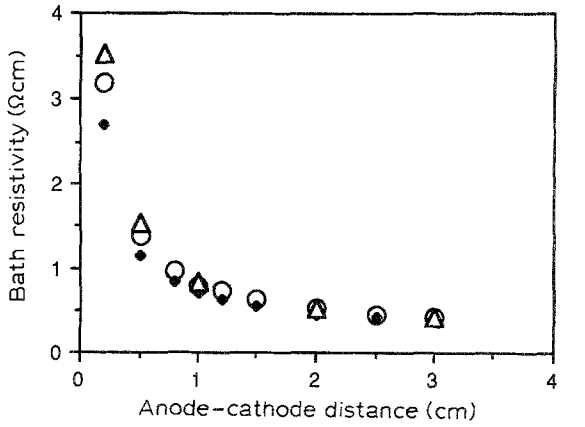

Fig. 1. Bath resistivity against *ACD* for anodes of different carbon materials. $[Al_2O_3]$ = 7.5 wt %, *CR* = 3.0, and *T* = 985° C. (○) Type I, (◆) Type II and (△) ⟨ATJ⟩.

jump for *ACD*'s lower than 1 cm, suggesting that the effective bath resistivity is significantly influenced by the low *ACD* settings. These also indicate the significance of bubble contribution to the effective bath resistivity [1, 2]. The values at the highest *ACD* (i.e. at 3 cm) which are least affected by the presence of bubble, compare favourably with the theoretical values presented earlier [6]. The bath resistivity values at one *ACD* indicate that Type I anode produces a higher bath resistivity than the Type II anode. Figure 1 shows the differences in bath resistivity values among Type I, Type II and ATJ graphite anodes when the alumina concentration was 7.5 wt %, *CR* was 3.0, and temperature was 985° C. After assuming an error of ± 1 mm in the ACD setting, a t-distribution analysis was performed on the bath resistivity values of the three anodes at each ACD. The results (at 95% significance) showed that Type II anode produces a lower bath resistivity value compared with those of the other two anodes. This would suggest that Type I anode produces bubbles with higher dynamic gaseous volume fraction, ε. One possible reason for this is the bubbles produced by anode Type I are smaller (which means they will travel more slowly) compared with those produced by the other anodes.

The values of bath resistivity at each *ACD* were normalized with respect to the bath resistivity value estimated from Choudary's equation [9] to give the ratio of bath resistivity. A summary of the bath resistivity values at relevant operating conditions have been presented in the previous paper [6]. Taking the case where alumina concentration was 7.5 wt %, *CR* was 3.0, and temperature was 985° C, a bath resistivity value of 0.4195 Ω cm is obtained. The values of the ratio of bath resistivity should indicate any change in the bubble contribution to the effective bath resistivity. (For an ideal case where there is no effect of bubbles on bath resistivity, a constant ratio of 1 would be expected at any *ACD*. Ratios greater than one are indicative of the increasing contribution of the bubble layer on the bath resistivity). Figure 2 and Table 3 summarize the values of ratio of both resistivity at the above bath composition. These values indicate that the bubble contribution to the effective bath resistivity increases as *ACD* is decreased. The two electrodes give the same trend. A comparison of the values at each *ACD* for the two electrode, however, shows that Type II anode gives rise to a lower bubble contribution to the bath resistivity than Type I anode, in agreement with the previous observation.

As further verification of the above observation, the

Table 2. Bath resistivity (Ω cm) at $[Al_2O_3]$ = 7.5 wt %, T = 985° C, with 5.5 wt % NaCl.

Electrode	Type I		Type II	
ACD (cm)	CR3*	CR213†	CR3*	CR213†
0.2	2.93	4.43	2.36	4.36
0.5	1.27	2.02	1.09	1.89
0.8	0.86	1.29	0.79	1.24
1.0	0.79	1.09	0.66	1.02
1.2	0.70	0.94	0.59	0.89
1.5	0.57	0.79	0.50	0.76
2.0	0.48	0.62	0.42	0.62
2.5	0.41	0.53	0.39	0.52
3.0	0.40	0.48	0.38	0.47

* CR3 = CR of 3.0.
† CR213 = CR of 2.13.

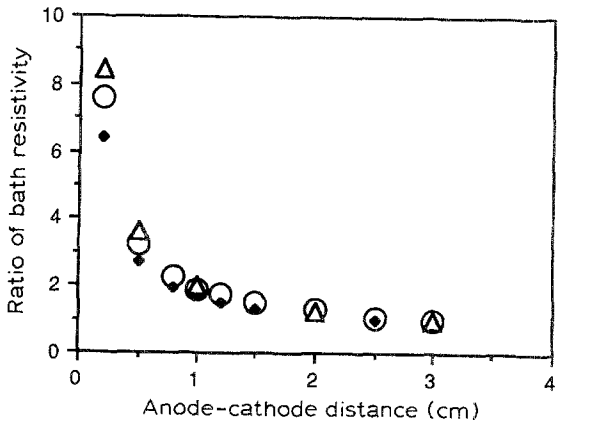

Fig. 2. Ratio of bath resistivity against *ACD* for anodes of different carbon materials. $[Al_2O_3]$ = 7.5 wt %, *CR* = 3.0, and *T* = 985° C. (○) Type I, (◆) Type II and (△) ⟨ATJ⟩.

Table 3. Ratio of bath resistivity (Γ/Γ_0) *at* Al_2O_3 = 7.5 wt %, *CR = 3.0, T = 985° C*

Electrode	*Type I*	*Type II*
ACD (mm)		
2	7.62	6.46
5	3.26	2.73
8	2.28	1.94
10	1.88	1.67
12	1.76	1.49
15	1.50	1.28
20	1.27	1.08
25	1.06	1.00
30	1.00	0.99

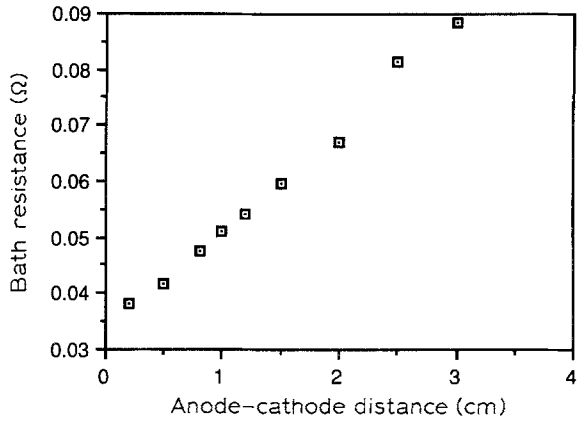

Fig. 3. Bath resistance against *ACD* plot for anode Type I [Al_2O_3] = 7.5 wt %, *CR* = 3.0, and *T* = 985° C.

bubble layer resistivity and gaseous volume fraction in the bubble layer were estimated by using the following analysis of the bath resistance data and assuming a bubble layer thickness of 1 cm.

The bubble layer resistivity and the gaseous volume fraction can be calculated from plots of total bath resistance R_T against *ACD*. The relationship of these two variables is outlined below, however, this was described in more detail in a separate paper [6].

The total bath resistance can be considered as the sum of the resistance of the bubble free region and that of the bubble layer, therefore can be written as:

$$R_T = (\Gamma_1 - \Gamma_2)\,\delta/A + (\Gamma_2/A)\,ACD \quad (1)$$

For illustration purposes, the Bruggemann's equation [11, 12] has been assumed to be applicable in this case,

$$\Gamma_1 = \Gamma_2\,(1 - \varepsilon)^{-1.5} \quad (2)$$

and that total bath resistance R_T is equal to ($\Gamma \cdot ACD/A$), then:

$$\Gamma = \Gamma_2\,[1 + (\delta/ACD)\{(1 - \varepsilon)^{-1.5} - 1\}] \quad (3)$$

where Γ = effective bath resistivity (Ω cm); Γ_1 = bath resistivity in the bubble layer (Ω cm); Γ_2 = bath resistivity in the bubble-free layer (Ω cm); δ = bubble layer thickness (cm); A = surface area of the anode (cm^2), which is assumed to be the electrolyte cross sectional area, assuming no Fanning effects; *ACD* = anode–cathode distance (cm); and R_T = total resistance from anode to cathode surface (Ω). Various other models, which can probably be applied for this case, have been discussed in another forum [13].

From a plot of R_T against *ACD*, therefore, bubble layer resistivity is calculated from the intercept, and thus gaseous volume fraction can also be determined from the Bruggemann's equation. A typical plot of R_T against *ACD* for one of the carbon electrode is shown in Fig. 3.

From the slope of this plot, and using the theoretical bath resistivity determined by Choudary's equation [10] one can determine the correction factor [6]. This correction factor can then be used to find the corrected bubble-layer bath resistivity and gaseous volume fraction. The need for a correction factor arises due to the facts that the effective bath area is not equal to the anode geometric surface area. The correction factor is basically the ratio of effective bath area to the geometric surface area.

The effective bath area can be estimated by using a method described by Haupin [13, 14] as in the following equation:

$$A_e = I/(e\tau_0) \quad (4)$$

where A_e = effective bath area under anode (cm^2) and equal to effective anode area; I = current through anode (A); τ_0 = electrical conductivity of the bath ($\Omega^{-1}\,cm^{-1}$); and e = voltage gradient in the bath under centre of the anode in the absence of bubbles ($V\,cm^{-1}$). Values of e were determined from the cell potential data at *ACD*s of 1 to 3 cm for each set of conditions, while τ_0 was estimated from Choudary's equation [10]. Values of A_e can then be calculated and the correction factor is obtained.

The calculated values of the bubble layer resistivity and the gaseous volume fraction of the bubble layer are summarized in Tables 4 and 5. For each of the melts studied the bubble layer resistivity is lower for the Type II anode than that of Type I. Except for experimental condition No. 3 in Table 4 the ATJ graphite produces the highest bubble layer resistivity values. The values of gaseous volume fraction given in

Table 4. Corrected bubble layer resistivity Γ_1 (Ω cm) *bubble layer thickness is 1 cm*

Electrode conditions	⟨*ATJ*⟩	*Type I*	*Type II*
1. *CR* = 3.0 Al_2O_3 = 7.5 wt % *T* = 985° C	1.6744	1.5810	1.1230
2. *CR* = 3.0 Al_2O_3 = 7.5 wt % *T* = 985° C NaCl = 5.5 wt %	1.8636	1.6790	1.1550
3. *CR* = 2.13 Al_2O_3 = 7.5 wt % *T* = 985° C NaCl = 5.5 wt %	2.1450	2.8880	2.5710

Table 5. Gaseous volume fraction in the bubble layer, ε, calculated by using Bruggemann's equation [9, 10]. Bubble layer thickness is 1 cm

Electrode conditions	*⟨ATJ⟩*	*Type I*	*Type II*
1. *CR* = 3.0 Al_2O_3 = 7.5 wt % *T* = 985° C	0.60	0.59	0.48
2. *CR* = 3.0 Al_2O_3 = 7.5 wt % *T* = 985° C NaCl = 5.5 wt %	0.64	0.61	0.50
3. *CR* = 2.13 Al_2O_3 = 7.5 wt % *T* = 985° C NaCl = 5.5 wt %	0.63	0.69	0.67

Table 6. Ratio of bath resistivity (Γ/Γ_0) at [Al_2O_3] = 7.5 wt %, T = 985° C, and NaCl = 5.5 wt %

Electrode	Type I		Type II	
ACD (mm)	*CR = 3*	*CR = 2.13*	*CR = 3*	*CR = 2.13*
2	7.22	9.04	5.83	8.91
5	3.13	4.12	2.68	3.85
8	2.11	2.64	1.95	2.53
10	1.94	2.22	1.62	2.09
12	1.72	1.91	1.46	1.83
15	1.41	1.61	1.23	1.56
20	1.18	1.27	1.03	1.26
25	1.01	1.08	0.97	1.06
30	0.97	0.99	0.93	0.97

Table 5 also show that anode Type II with a lower gas volume fraction would produce a smaller bubble contribution to the bath resistivity than anode Type I.

3.2. *Effect of bath composition*

The addition of 5.5 wt % NaCl to the bath is expected to reduce the effective bath resistivity as it increases the melt conductivity [10]. This is consistent with the experimental results (at *ACD* = 30 mm) shown in Table 1. Following the same procedure as above, the values of the bubble layer resistivity and gaseous volume fraction were determined before and after the addition of 5.5 wt % NaCl to the bath. Tables 4 and 5 indicate that changes in the bubble contribution to the effective bath resistivity with the addition of NaCl are relatively small.

AlF_3 was also added to the above melt to study the effect of varying *CR*. Since NaCl was present in the bath, the observed effects are actually the effects of excess AlF_3 in the presence of 5.5 wt % NaCl. Consistent with prediction from Choudary's equation the lower *CR* of 2.13 lowers the conductivity of the bath, and therefore increases the effective bath resistivity (as shown in Table 2). The values of the ratio of bath resistivity at each *ACD* are presented in Table 6. The bubble contribution to the bath resistivity is lower at the higher *CR*. It can thus be concluded that the rise in the effective bath resistivity is caused by a reduction in the bath conductivity as well as by an increase in the bubble contribution.

4. Conclusions

The differences in the bath resistivity values obtained in this study for different anode materials show that the carbon can influence the bubble contribution to the effective bath resistivity by affecting the nature of the CO_2 bubbles produced during electrolysis. The two most likely causes of this phenomenon are differences in bubble size produced by different anode materials, and differences in wetting behaviour of the anode materials. Verification of the phenomena requires physical observation of the bubbles which was not possible in the present study. The present results show that Type II anode with the larger fines fraction and more porous appearance produces bubbles which gives a lower effective bath resistivity compared with both the ⟨ATJ⟩ graphite anode, and Type I anode which had the optimum granulometry and pitch content.

The results of this study also confirm earlier findings [1, 2, 6] that:

(i) the *ACD* setting influences the effective bath resistivity. This effect becomes more significant as ACD is decreased because the CO_2 bubble contribution increases with decreasing *ACD*.

(ii) The addition of excess AlF_3 (from *CR* = 3 to *CR* = 2.13) to the bath with 5.5 wt % NaCl and 7.5 wt % alumina at 985° C increases the bath resistivity by decreasing its specific conductivity. The bubble contribution to the effective bath resistivity was also observed to increase with this change in *CR*.

(iii) Addition of 5.5 wt % NaCl to the bath with *CR* = 3, 7.5 wt % alumina and *T* = 985° C results in a reduction in the melt's specific resistivity. Changes in the bubble contribution were small and considered insignificant however, as they were within the experimental limitations.

The present results also confirm that the bath resistance analysis method described in detail earlier [6] can be used to estimate the bubble layer resistivity Γ_1 and also the gaseous volume fraction of this bubble layer, ε.

References

[1] D. Kasherman and M. Skyllas-Kazacos, *J. Appl. Electrochem.* **18** (1988) 863–8.

[2] D. Kasherman and M. Skyllas-Kazacos, *CHEMECA'88*, 1, pp. 268–73, Sydney, 28–31 August 1988, Australia.

[3] J. R. Payne, U.S. Patent 4 093 524 (1978).

[4] R. C. Doward, *J. App. Electrochem.* **13** 569–75 (1983).

[5] K. Grjotheim, C. Krohn, M. Malinovsky, K. Matiasovsky and J. Thonstad, 'Aluminium Electrolysis', Aluminium Verlag GmbH, Dusseldorf (1982).

[6] D. Kasherman and M. Skyllas-Kazacos, 'Determination of Bubble layer Resistivity and Gaseous Volume Fraction

in an Aluminium Electrolysis Cell with Sloping Anode and Cathode', *ALUMINIUM International Journal*, in press.
[7] G. J. Houston, 'Anodic Evolution and Dissolution of Chlorine in Melts Containing Aluminium Chloride', *Master of Science Thesis*, University of New South Wales, Sydney, Australia (1977).
[8] A. Solheim and J. Thonstad, '*Light Metals 1986*', 115th Annual Meeting of AIME (1986) pp. 397–403 and '*Light Metals 1987*', 116th Annual Meeting of AIME (1987) pp. 239–45.
[9] D. Kasherman and M. Skyllas-Kazacos, *Proceedings of the 7th Australian Electrochemical Conference* (edited by Skyllas-Kazacos) University of New South Wales, Kensington, N.S.W. (1988) pp. 183–6.
[10] G. Choudary, *J. Electrochem. Soc.* **120** (1973) 381–3.
[11] H. Vogt, *J. Appl. Electrochem.* **13** (1983) 87–8.
[12] P. J. Sides, 'Modern Aspects of Electrochemistry, No. 18' (edited by R. E. White, J. O'M. Bockris and B. E. Conway) pp. 303–54, Plenum Press, New York (1986).
[13] D. Kasherman, PhD Thesis, University of New South Wales, Kensington, N.S.W. (1989).
[14] W. E. Haupin, *J. Metals* **10** (1971) 46–9.